NJC

A Membrane Penetrating Cyclic Lipopeptide Based Nanocarrier for Cancer Drug Delivery

Journal:	*New Journal of Chemistry*
Manuscript ID	NJ-ART-10-2024-004643.R2
Article Type:	Paper
Date Submitted by the Author:	14-Mar-2025
Complete List of Authors:	Zhang, Wenjie; Binzhou Medical University, Department of Pharmacy Science Luo, Junlin; Binzhou Medical University, Department of Pharmacy Science Sun, Jingyang; Binzhou Medical University, Department of Pharmacy Science Chen, Weixi; Binzhou Medical University, Department of Pharmacy Science Wei, Guangcheng; Binzhou Medical University, Department of Pharmacy Science Yan, Miaomiao; Binzhou Medical University, Department of Pharmacy Science

A Membrane Penetrating Cyclic Lipopeptide Based Nanocarrier for Cancer Drug Delivery

Wenjie Zhang[#], Junlin Luo[#], Jingyang Sun, Weixi Chen, Guangcheng Wei[*] , Miaomiao Yan[*]

Department of Pharmacy Science, Binzhou Medical University, Yantai 264003, China

[#] The contribution of these authors is equal.

E-mail: weiguangcheng2004@126.com; yanmm81@163.com

Abstract:

Herein, a cyclic lipopeptide CLP5 with a 1,3,4-oxadiazole and tertiary amine structure was developed to address issues in tumor chemotherapy like non-specificity, drug resistance, and poor bioavailability. The CLP5 not only exhibited anticancer activity through membrane breaking and targeting caspase-3, but also self-assembled into stable spherical aggregates which encapsulated doxorubicin to form CLP5@DOX nanomedicine. The encapsulation efficiency of doxorubicin was 81.46±3.23%. The release of DOX from the CLP5@DOX nanomedicine exhibited sustained release and pH responsiveness. In vitro experiments showed that CLP5@DOX nanomedicine not only had high penetrating membrane activity to induce cancer cell apoptosis, but also had low toxicity and high serum stability. Animal experiments showed that CLP5@DOX nanomedicine could effectively inhibit tumor growth while reducing the adverse reactions and toxicity of DOX. Molecular docking experiments showed that CLP5 could activate the caspase-3 to target the apoptosis pathway. In conclusion, CLP5 has high potential as a drug carrier for clinical cancer treatment.

Key words: cyclic peptide, lipopeptide, nanomedicine, antitumor

1. Introduction

The treatment methods for cancer mainly include chemotherapy, radiotherapy, surgery and immunotherapy. Chemotherapy is the primary treatment method, but traditional chemotherapy drugs can cause serious adverse reactions and toxicity. Therefore, the development of new anti-tumor drugs is urgent[1-4]. Anticancer peptides are considered to be a new generation of anti-tumor drugs due to their diversity in structure and

function[5-8].

The anticancer activity of polypeptides can be significantly enhanced by introducing imidazole heterocycles into the peptide skeleton[9]. 1,3,4-oxadiazole is a biologically important scaffold with various biological activities. Research has shown that 1,3,4-oxadiazole and its derivatives have strong anticancer activity in the treatment of cancer[10-11]. As an internal control element, 1,3,4-oxadiazole not only stabilizes the secondary structure of cyclic peptide molecules, but also promotes the formation of intramolecular hydrogen bonds, reducing the polar surface area and improving cell membrane permeability[12-14]. In addition, 1,3,4-oxadiazole derivatives can activate caspase-3, which is overexpressed in various human cancers[15]. Therefore, 1,3,4-oxadiazole derivatives can target apoptosis pathways and induce cancer cell apoptosis[16-17]. In addition, modification of fatty acids can increase the membrane permeability, anticancer activity, and prolong the circulation time in the body[18].

Doxorubicin is a traditional chemotherapy drug that has good therapeutic effects on solid tumors, but its clinical application is limited by severe toxic side effects[19]. The drug delivery system based on the polypeptides can passively target the drug to the tumor site by enhancing permeability and retention (EPR) effect, and increase the effective concentration of the drug (DOX) at the tumor site and reduce the toxic side effects of the drug[20-25], and exert the combined anti-tumor effect, and which further overcome the drug resistance.

Herein, the line peptide P5 was firstly designed and synthesized, and then 1,3,4-oxadiazole and tertiary amine structures were introduced into the P5 peptide using (N-isocyanoamino) triphenylphosphane to form a cyclic peptide CP5. Meanwhile, cyclic lipopeptide CLP5 was synthesized through the conjugation of CP5 and n-octanoic acid to further improve the in vivo stability and anticancer activity of CP5. CLP5@DOX nanomedicine was prepared through the encapsulation of CLP5 aggregates to DOX, and which could overcome the resistance and reduced toxic side effects of DOX, and exerted the combined anti-tumor effect of CLP5 and DOX as shown in **scheme 1**.

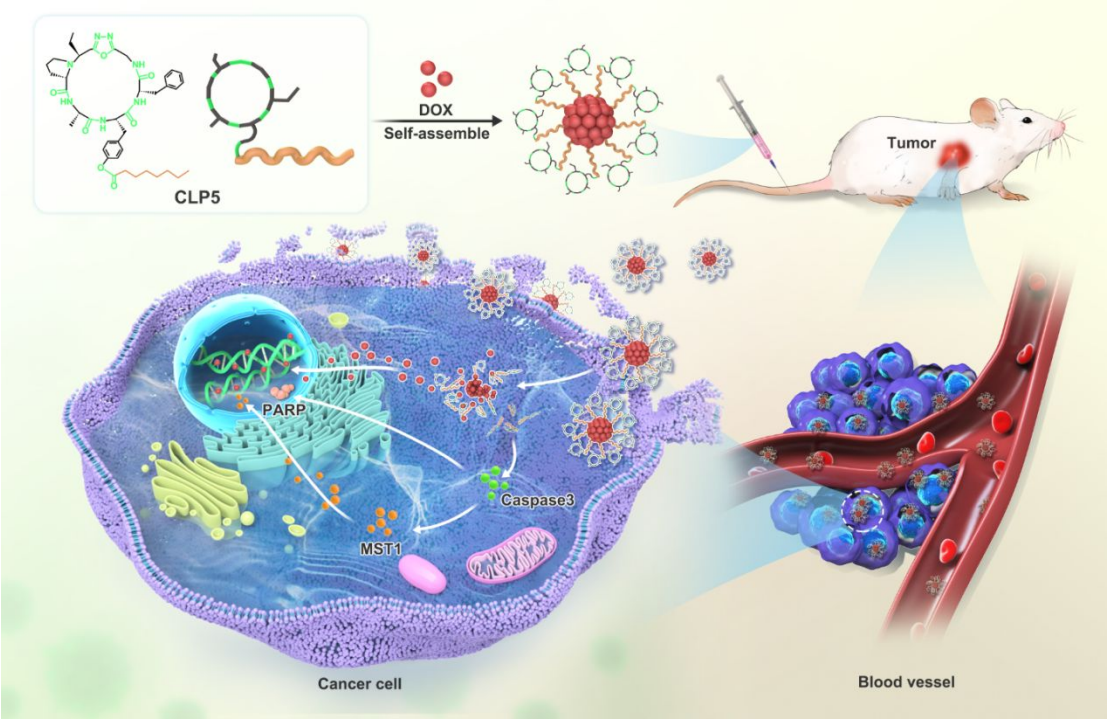

Scheme 1. Heterocyclic lipopeptide CLP5 based on the oxadiazole structure self-assembles into spherical aggregates and encapsulates doxorubicin, which exerts a combined antitumor effect by targeting caspase-3 and penetrating membrane.

2. Experiment

2.1 Synthesis of CLP5 cyclolipopeptide

2.1.1Synthesis of P5 linear peptide

Herein, the P5 peptide (NH-Pro-Ala-Tyr(tBu)-Phe-Gly-COOH) was synthesized with the method of solid phase synthesis. The resin was firstly activated, and CTC resin-Gly-Fmoc (10.0 g, and the loading amount is 0.347 mmol·g^{-1}) was dispersed into the anhydrous DMF to swell for 30 minutes（25℃）, and then ninhydrin was used to detection, and the next reaction step can be processed if the solution is colorless. Then add 20% piperidine to remove the Fmoc protective group. Then filtered, and successively washed with DMF, DCM (Dichloromethane) and DMF for 5 times, and then re-swelled for 30 minutes in anhydrous DMF, and then Fmoc-Phe-OH (2.855 g), DCC (1.862 g), HOBT (1.219 g) and DIEA (1.49 mL) were added to react with stirring for 48 hours. Then filtered, and successively washed with DMF, DCM and DMF for 5 times, and then dialyzed (MW8000-14000) with anhydrous ethanol for about 40 times (Every time was about 30 minutes), then the CTC resin-Gly-Phe-Fmoc was obtained through the freeze drying. The Fmoc-Tyr(tBu)-OH, Fmoc-Ala-OH and Fmoc-Pro-OH

were successively conjugated to obtain the CTC resin-Gly-Phe-Tyr(tBu)-Ala-Pro-NH sample according to the same procedure. The CTC resin-Gly-Phe-Tyr(tBu)-Ala-Pro-NH sample was added to the cutting solution (The volume ratio of TFA to DCM was 1 to 99) with stirring for 1.5 hours to remove the CTC resin. After the prescribed time, add saturated sodium bicarbonate solution to extract and collect the organic phase, and the organic phase was condensed to 5 mL, and then poured into glacial ether (40 mL), and the precipitates was collected, and washed with ether for many times, and the P5 peptide (NH-Pro-Ala-Tyr(tBu)-Phe-Gly-COOH) was obtained without further purification (**Scheme 2**). The molecular weight of P5 was further confirmed using a mass spectrometer(5800 MALDI-TOF/TOF, AB Sciex, USA).

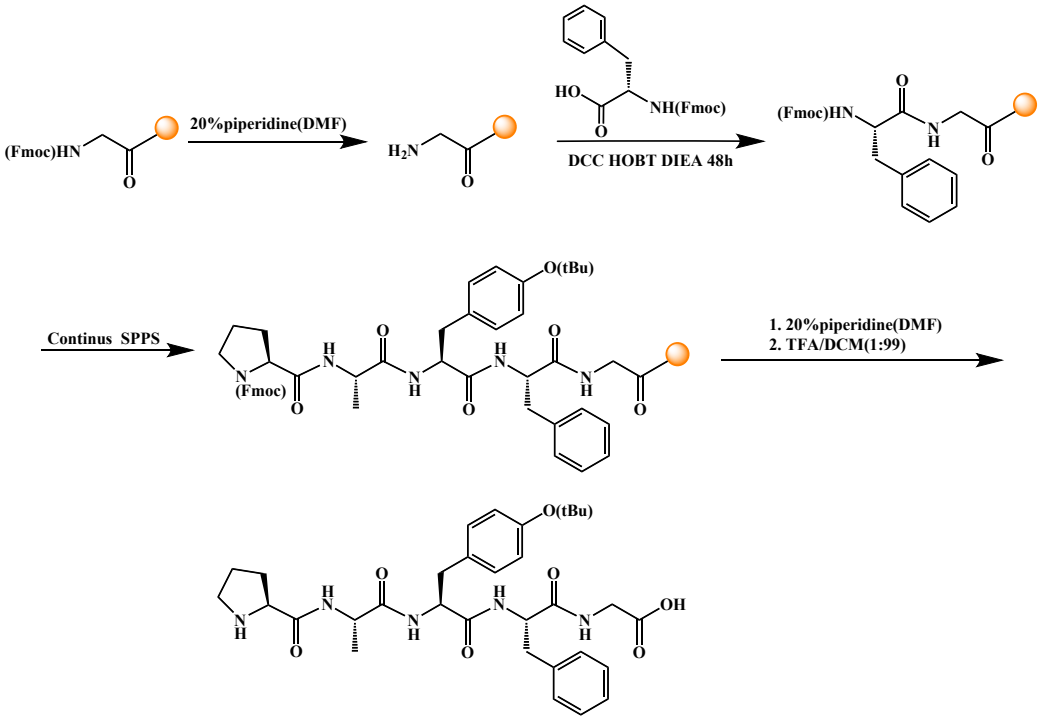

Scheme 2. Synthesis of P5 peptide.

2.1.2 Synthesis of CP5 cycle peptide

The cycle peptide CP5 (CP5) was synthesized through the macrocyclization reaction of P5, propionic aldehyde and (N-isocyanimino) triphenylphosphorane (**Scheme 3**). The P5 peptide was firstly suspended in a 1:1(V/V) mixture of DCM and acetonitrile (DCE:MeCN) with stirring, and the propionaldehyde(1.5 equiv) was added to the suspension followed by (N-isocyanimino) triphenylphosphorane (1 equiv) with stirring for 24 hours at 50 ℃. After the prescribed time, the crude CP5 sample was obtained

after removing the solvent. The crude sample was purified with the 8:2(V/V) eluent solution of petroleum ether and ethyl acetate (Petroleum ether: ethyl acetate) and Al_2O_3 (200 mesh) solid phase to obtain the pure CP5 sample. The molecular weight of CP5 was further confirmed using a mass spectrometer (5800 MALDI-TOF/TOF, AB Sciex, USA).

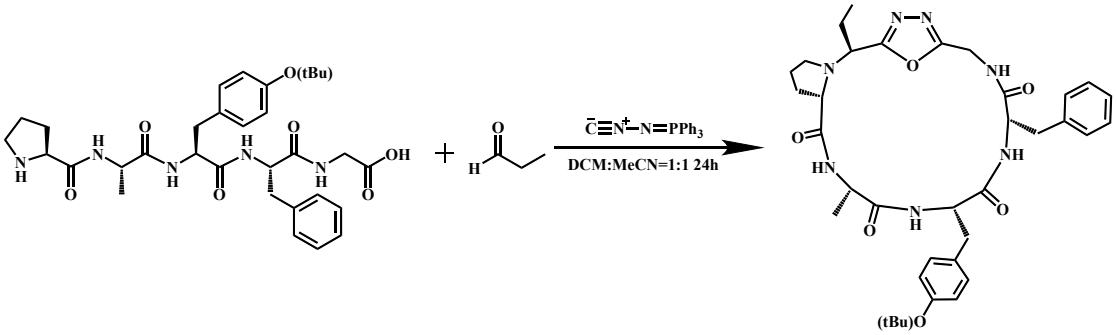

Scheme 3. Synthesis of CP5 cyclic peptide.

2.1.3 Synthesis of CLP5 cyclic lipopeptide

The cycle lipopeptide CLP5 was synthesized through the etherification reaction of CP5 with the octanoic acid (**Scheme 4**). The hydroxyl protective group of CP5 was firstly removed with the cutting solution (TFA:Tis:H_2O=95:2.5:2.5， V/V/V) with stirring for 1.5 hours, and then concentrated the solution by vacuum distillation, and then the solution was precipitated with glacial ether, and then centrifugated (7000 rpm, 10min) to obtain the solid sample, and washed for many times with the glacial ether, and the sample was obtained after the ether evaparation. The octanoic acid, DCM, EDC, DMAP and DIEA were added the above sample with stirred reaction for 12 hours. Then crude sample was obtained after removing the DCM, and then purified with the 1:1 eluent solution of petroleum ether and ethyl acetate (Petroleum ether:ethyl acetate) and Al_2O_3 (100-200 mesh) solid phase to obtain the pure CLP5 sample. The molecular weight of CLP5 was further confirmed using a mass spectrometer (5800 MALDI-TOF/TOF, AB Sciex, USA).

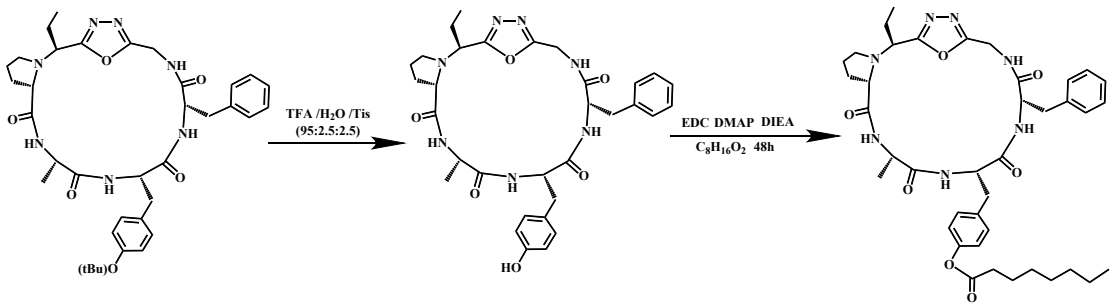

Scheme 4. Synthesis of CLP5 cyclic lipopeptide.

2.2 Characterization of aggregate morphology and particle size distribution.

The CLP5 cyclic lipopeptide has the ability to self-assemble and form aggregates in aqueous solution. A drop of aggregates solution was dropped to the copper mesh with carbon supporting membrane for 2 minutes, and the excessive solution was removed from the side of the copper mesh. Then a drop of phosphotungstic acid (1%) was dropped to the copper mesh for 2 minutes, and the excessive solution was removed with filter paper, and the copper mesh was irradiated with the infrared lamp for 5 minutes to make the copper mesh dry, and then the morphology of CLP5 aggregates was observed with the TEM (Transmission electron microscopy, JEM-1400, JEOL, JPN). And the CLP5 aggregates size and Zeta potential were determined with the Malvin particle size analyzer (Zeta sizer Nano ZSP, England).

2.3 The preparation of CLP5@DOX nanomedicine

DOX·HCl (DOX, 1.0 mg) was dissolved into the methanol solution (10 mL, containing the 480 mL triethylamine) with stirring for 24 hours under darkness. The CLP5 (1.0 mg) was dissolved into the methanol, and then the above two solutions were mixed, and incubated for 30 minutes at 50℃, the methanol was evaporated using vacuum distillation, and the distilled water was added to disperse the sample, and centrifugated to obtain the precipitates which was the CLP5@DOX nanomedicine. Solution was the free DOX aqueous solution, and the free DOX concentration could be obtained according to the standard absorbance curve at 480 nm. The encapsulation efficiency (EE) of CLP5 aggregates to DOX could be calculated with the following formula:

$$EE\% = \left(1 - \frac{Csup}{Ctol}\right) \times 100\%$$

Csup is the concentration of free DOX in supernatant; Ctol is the total

concentration of DOX.

2.4 CLP5@DOX nanomedicine release behavior *in vitro*

The DOX release behavior in vitro was simulated with the four different buffer solutions (pH=7.4 PBS, pH=5.0 PBS, pH=7.4 10% FBS and pH=5.0 10% FBS). Firstly, the CLP@DOX nanomedicine was dissolved in the buffer solution and then added to the dialysis bag (Molecular weight cutting-off of dialysis bag: 2000 Da). The dialysis bag was placed in 20 mL of buffer solution of pH 7.4 and pH 5.0 PBS and 10% FBS at 37°C for release experiments. At 1 h, 4 h, 12 h, 24 h, 36 h, 48 h, 60 h, and 72 h, 4 mL of dialysate was taken out, and 4 mL of fresh dialysis medium was added to maintain the same volume of the solution. Measure the absorbance of the dialysis medium using a UV-visible spectrophotometer at a wavelength of 480 nm.The accumulated amount was calculated with the following formula:

$$\text{Accumulated release percentage} = (n_i C_i V + \sum n_{i-1} C_{i-1} V_{extract})/W \times 100\ \%$$

n_i is the taken sample times; C_i is the concentration of every taken sample; V is the PBS totalvolume (20 mL); V_{extrac} is the taken sample volume (4.0 mL); W is the DOX total amount.

2.5 Cell culture

The HepG2 cells and H22 cells selected for this experiment were obtained from the Medical Research Center of Binzhou Medical University. HepG2 and H22 cells were inoculated into the culture dish and high sugar medium containing 10% fetal bovine serum and 1% double antibody was added respectively, and then incubated in an incubator containing 5%CO_2 at 37℃ for overnight. Cells with good growth status were selected for the experiment.

2.6 *In vitro* anticancer activity

The MTT method was used to evaluate the anticancer activity of CLP5 and CLP5@DOX nanomedicine with the HepG2 cell line. The HepG2 cells (About 2000 cells) were inoculated into the 96-well for culture 24 hours to make the cells adherent to the wall, and removed the old culture medium. Then the fresh medium contained CLP5, DOX and CLP@DOX were added into the 96-well respectively (The concentration was 0 $\mu g \cdot mL^{-1}$, 20 $\mu g \cdot mL^{-1}$, 40 $\mu g \cdot mL^{-1}$, 60 $\mu g \cdot mL^{-1}$, 100 $\mu g \cdot mL^{-1}$

and 120 μg·mL^{-1} respectively) for 24 hours and 48 hours incubation respectively. Then 20 μL MTT (5 μg·mL^{-1}) was added for another 4 hours incubation, and removed the supernatant, and DMSO (150 μL) was added into each well to dissolve the crystal under the darkness to avoid the light irradiation, and shaken for 5 minutes at 120 r·min^{-1}, and the OD values were determined with the microplate reader at 485 nm. The relative cell viability was calculated according to the following formula with the absorbance intensity to obtain the anticancer activity of CLP5 and CLP5@DOX nanomedicine.

Relative cell survival rate = [(As-Ab) /(Ac-Ab)]×100%

As: The absorbance intensity of sample group; Ac: The control group; Ab: The blank group.

RAW 264.7 cells were selected to analyze the cytotoxicity of CLP5 cyclic lipopeptide with the same experimental method.

2.7 Serum stability test

In order to evaluate the CLP5 stability in serum, CLP5 were firstly co-cultured with 10% fetal bovine serum (FBS), and then the anti-cancer activity of CLP5 was tested with the MTT method. CLP5 were pre-incubated with 10% FBS and PBS for 24 hours and 48 hours separately. When the density of HepG2 cells in Petri dish reached about 90%, the cells were digested with trypsin and inoculated into 96-well plates (About 2000/well), and incubated for 24 hours. Then removed the old culture medium, and the CLP5 solution (CLP5 after co-culture with 10% fetal bovine serum (FBS)) was added for another 24 hours incubation. After the prescribed time, MTT (20 μL, 5mg·mL^{-1}) was added to each well respectively, and incubated for 4 hours at the incubator, and removed the supernatant, then DMSO (150 μL) was added into each well and shaken (160 r·min^{-1}) for 8 minutes, and the absorbance intensity was determined with the microplate reader at 485 nm, and then the relative cell viability was obtained. Cell relative viability = [(As-Ab) /(Ac-Ab)]×100%

As: The drug group; Ab: The blank group; Ac: The control group.

2.8 Activity study of penetrating cell membrane

2.8.1 The experiment of PI/Hoechst33342 staining

The HepG2 cell line was used for the PI/Hoechst33342 experiment. HepG2 cells in logarithmic growth phase were harvested by trypsinization (0.25% trypsin-EDTA, 37℃, 3 min) and resuspended in complete DMEM medium (10% FBS, 1% penicillin/streptomycin). HepG2 cells in logarithmic growth phase were inoculated into a 6-well plate. After HepG2 cells adhered to the wall, GLP5 was co-cultured with HepG2 cells for 5 minutes and 30 minutes, respectively, and then removed the old culture medium, and fresh culture medium containing propidium iodide (PI) and Hoechst33342 (The final concentration of PI was 50 $\mu g \cdot mL^{-1}$, Hoechst33342 with a final concentration of 5 $\mu g \cdot mL^{-1}$) were added, and then incubated in the 6-well plate in an incubator for 5 minutes, then rinsed twice with PBS solution. Finally, the cell morphology was observed with the fluorescence microscope.

2.8.2 LDH releasing experiment

LDH (lactate dehydrogenises) is a stable soluble enzyme that exists in the cytoplasmic matrix. When cell apoptosis or necrosis occurs, the cell membrane is destroyed, and LDH is released into the culture medium. Therefore, the cell membrane penetrating ability of CLP5 can be measured quantitatively using an LDH kit. HepG2, which is in the logarithmic growth phase, was inoculated into a 96-well plate and cultured for 24 hours. Then, different concentrations of CLP5 solutions (without serum) were added for another 24 hours. TritionX-100(1%, V/V) was added to incubation for 1 h, then centrifuged (400 $r \cdot min^{-1}$) for 5 minutes. The supernatant was transferred to a new 96-well plate, and LDH solution (60 μL) was added to each well for 30 minutes incubation in dark, and then the OD values were measured at 490 nm, and the 1% tritionX-100 was used as a positive control group. The LDH releasing amount was calculated using the following formula.

$$LDH\ (\%) = (ODi - ODn) / (ODp - ODn) \times 100\%$$

ODi: The absorbance intensity of the experiment group; ODp: The absorbance intensity of the positive control group; ODn: The absorbance intensity of the negative control group.

2.9 Cell uptake

2.9.1 Laser Scanning Confocal Microscopy (LSCM)

The LSCM was used to observe the uptake of HepG2 cells to CLP5@DOX nanomedicine. The HepG2 cells were recovered to a Petri dish, and incubated for 24 hours to make the HepG2 cells adhere to the wall. Then the HepG2 cells were inoculated into a dish which was used for LSCM observation, and CLP5@DOX nanomedicine dispersion solution (2 mL, 10 $\mu g \cdot mL^{-1}$) was added for incubation 4 h, 8 h and 24 h. After the prescribed time, the old medium was removed, and washed with PBS (1×) three times, and 2 mL of fresh culture medium was added, and then the cell uptake was observed with the LSCM (Excitation wavelength was 488 nm, and the emission wavelength was 590 nm).

2.9.2 Flow cytometry (FCM)

The uptake of HepG2 to CLP5@DOX nanomedicine was also quantitatively determined with flow cytometry (FCM). The HepG2 cells were firstly inoculated into the 6 well plates, and the culture medium (2 mL) was added, and then was incubated for 24 hours. After the prescribed time, the old culture medium was removed, and CLP5@DOX nanomedicine dispersion solution (2 mL, 20 $\mu g \cdot mL^{-1}$) was added for incubation 4 h, 8 h and 24 h respectively, and the supernatant in each well was removed, and washed with PBS for 3 times. Then the trypsin (1 mL) was added to each well to digest the cells. Then the supernatant was removed through the centrifugation for 5 minutes (1000 $r \cdot min^{-1}$, room temperature), and PBS (1×, 0.5 mL) was added to the centrifuge tube to re-suspend the cells, and then the re-suspended cell was transferred to the FCM tube for FCM testing (Excitation wavelength was 488 nm, and the emission wavelength was 590 nm).

2.9.3 The mechanism of cell uptake

The frozen HepG2 cells was firstly resuscitated into a culture dish and cultured in an incubator at 37 ℃， and then the HepG2 cells in the logarithmic growth phase were seeded in the 6-well plates. The culture solutions (2 mL) was separately added the negative control group, the positive control group and the group of cell uptake inhibitors which were amiloride(20 $\mu g \cdot mL^{-1}$), chlorpromazine(20 $\mu g \cdot mL^{-1}$) and methyl-β-cyclodextrin(20 $\mu g \cdot mL^{-1}$) for 1h incubation. After the prescribed time, the

culture solutions (2 mL) which contained the CLP5@DOX nanomedicine(10 μg·mL^{-1}) were separately added into the positive control group, amiloride group, chlorpromazine group and methyl-β-cyclodextrin group for another 3h incubation, and the negative group was added into the culture solution (2 mL) for 3h incubation.

Then the culture solution was removed, and washed three times with the PBS(2 mL every time). The cells was digested with the trypsin(1 mL) for 1 min , and the culture medium (1 mL) was used to terminate the digestion for 1 min.The cells was collected and the supernatant was removed through the centrifuge(1000 R/min) for 5 min. The cells was re-suspended with the PBS (0.5 mL) and transfered to the tube of FCM for the FCM analysis(The excitation wavelength was 488 nm and the emission wavelength was 590 nm).

2.10 I*n vivo* anti-tumor activity

The mice model bearing tumor were constructed to evaluate the anti-tumor activity of CLP5 and CLP5@DOX nanomedicine, and the mice (20-25g) used in the experiment were all female Kunming white mice, and the animal experiments were executed according to the rules of "Guidelines for Care and Use of Animal Experiments" under the supervision of Binzhou Medical University(SYXK20210036) which was approved by the Department of Science & Technology of Shandong Province. The hemolysis experiment was executed to evaluate the hemolytic toxicity of CLP5 and CLP5@DOX nanomedicine, and the CLP5 (100 μL,2.25 mg·mL^{-1}) and CLP5@DOX nanomedicine (100 μL,2.25 mg·mL^{-1}) were injected into the mice body through the tail vein injection respectively, and the normal saline (NS, 100 μL) was used as the control group. After 2 hours, the mice blood was collected into the anticoagulant tube from the mice orbit, and then diluted with the NS for the morphology observation of red blood cells under the microscope.

The H22 cells (About 1×10^6) were subcutaneously injected into the left armpits of the mice. The mice were randomly divided into 4 groups when the tumor volume grew about 150-220 mm^3, and which were NS group, DOX group, CLP5 group and CLP5@DOX nanomedicine group. The above mice were administered by tail vein injection with the dosage of 100 μL each time. The interval between injections in each

group was 1 day, and a total of 4 times were required, the total time was 9 days. The mice body weight and tumor volume were determined before every injection. After the experiment, the mice were killed using cervical dislocation method for further experiments.

HE (Hematoxylin-eosin) staining can provide a more intuitive observation of CLP5 and CLP5@DOX nanomedicine on tumors, heart, liver, spleen, lungs, and kidneys in mice. The mice tumors, hearts, livers, spleens, lungs and kidneys were firstly immersed in 4% paraformaldehyde solution to fix for 24 hours. Then the tumor and other tissues were washed. The tumor and other tissues were gradient-eluted with ethanol solutions of varying concentrations. Then the tissues were embedded into the paraffin wax with tissue embedding machines, and sliced with the tissue slicer (0.5 μm). The deparaffinization process was performed by heating the samples at 50-60°C for 1.5 hours, followed by ethanol treatment (100% anhydrous ethanol) to dissolve the embedded paraffin. The sequential protocol was repeated twice to ensure wax removal. Tissue slices were stained with the hematoxylin and eosin. Finally the tissue slices were sealed with the neutral size, and the tissue slices were observed with the fluorescence microscopy.

2.11 Molecular docking of caspase-3 and CLP5 cyclic lipopeptide

The 3D structure of CLP5 was converted with the Chemdraw 3D software. The crystal structure of caspase-3 was obtained from the protein database (http://www.rcsb.org/PDB). The molecular docking of CLP5 and caspase-3 was completed via HDOCK SERVER[26]. Finally, PyMOL software was used to analyze and visualize the results of molecular docking.

2.12 Statistic analysis

Quantitative data is represented as mean value ± standard deviation (SD). The method of student's t-test was used to statistically analyze the data, and SPSS V26 software was used for analysis. Statistical significance is defined as * $p<0.05$ and ** $p<0.01$.

3. Results and discussion

3.1 Design and characterization of CLP5

The cyclization of peptides reduces conformational flexibility, thereby improving their

metabolic stability, binding affinity, and specificity with target molecules.The oxadiazole group was used to cyclize the P5 peptide, and the CP5 peptide has a highly conserved conformational geometry, where oxadiazole and tertiary amine contribute to conformational stability, forming a cyclic peptide with a rigid structure. 1,3,4-oxadiazole and tertiary amine act as inner ring control elements, promoting and stabilizing the hydrogen bonding network within the molecule. In addition, oxadiazole also promotes the passive membrane permeability of the cyclic peptide and improves its biological activity. The n-octanoic acid was conjugated with the CP5 to form the CLP5 which enhanced the cell membrane permeability, and further resulted in better biological activity.

The characterization of mass spectra was used to verify the synthesis of P5, CP5 and CLP5. The theoretical molecular weight of the linear pentapeptide P5 was 553.25, and as shown in **Figure 1a**, the negative ion peak of the P5 mass spectrum was 552.05, which was consistent with the theoretical molecular weight of the P5, indicating that the P5 had been synthesized. **Figure 1b** shows the mass spectrum of the cyclic peptide CP5, and the theoretical molecular weight of the P5 was 617.70, and the fragment ion peak after the loss of one carbon and two nitrogen atoms (-CN_2-) is 578.79, which was consistent with the molecular weight of the CP5, indicating that the CP5 has been synthesized. **Figure 1c** and **Figure 1d** showed the mass spectra of the negative ion mode ([M+Cl^-], **Figure 1c**) and positive ion mode ([M+NH_4^+], **Figure 1d**) of the cyclic lipopeptide CLP5 respectively. The theoretical molecular weight of the CLP5 was 743.90, which was consistent with that of the mass spectrum of the CLP5, indicating that the CLP5 has been synthesized.

The morphological characteristics of the self-assembled aggregates by cyclic lipopeptide CLP5 in water were observed with the TEM, and the particle size and *Zeta* potential of the CLP5 aggregates were determined with the Marvin particle size analyzer. The CLP5 aggregates are spherical in shape, with a relatively uniform particle size and complete morphology, evenly distributed, and no aggregation phenomenon occurs (**Figure 1e**). Seen from **Figure 1f**, the average particle size of CLP5 aggregates in aqueous solution was about 40 nm which make the CLP5 has the EPR effect. Due to

the obstruction of lymph reflux in tumor tissue, the retention time of CLP5 aggregates in tumor tissue is prolonged, providing a basis for passive tumor targeting. It is generally believed that aggregates particle sizes within the range of 20-200 nm have an EPR effect. The particle size of the CLP5 aggregate measured by the Marvin particle size analyzer was approximately 43.3 nm, with a *Zeta potential* of 10.3 mv(Figure S1a) in aqueous solution and a polydispersity index of 0.345, which indicated that the aggregate could maintain good dispersibility in aqueous solution. The CLP5 aggregates with positive charges, which can combine with negatively charged cancer cells through electrostatic interactions and exert anti-tumor effects. The *Zeta* potential of CLP5@DOX is +30.9mV(Figure S1b), and the following experiment also proved that the CLP5 aggregates could be used as an excellent drug carrier.

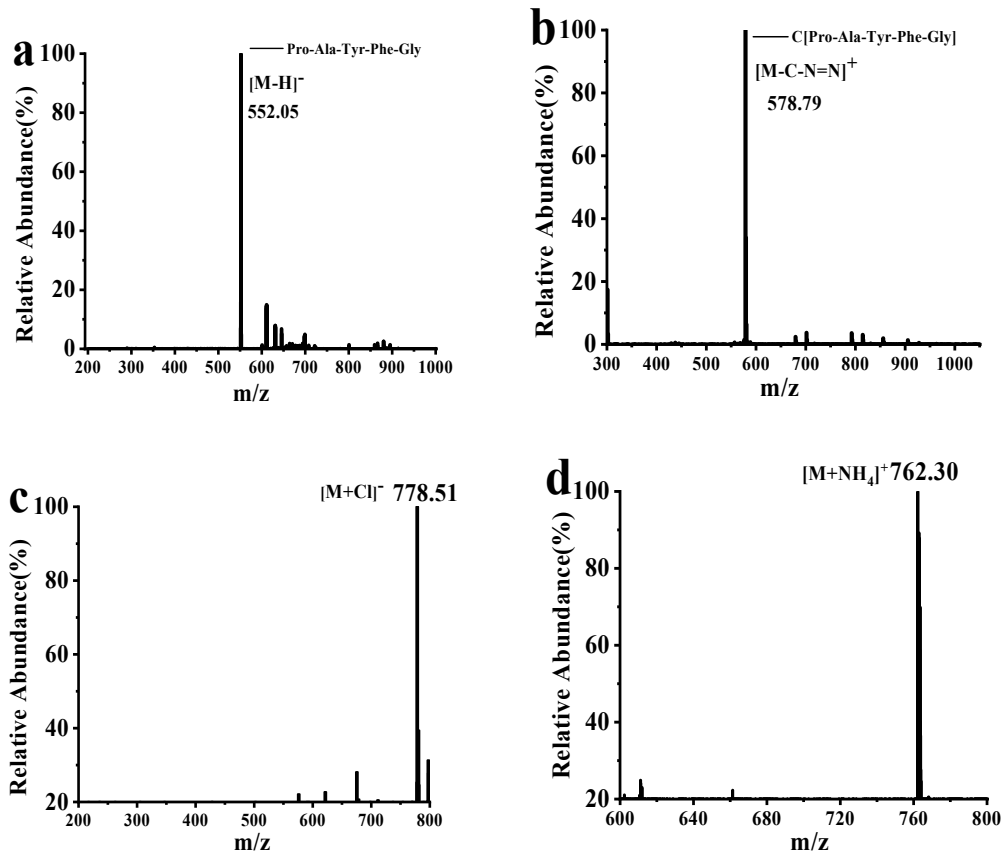

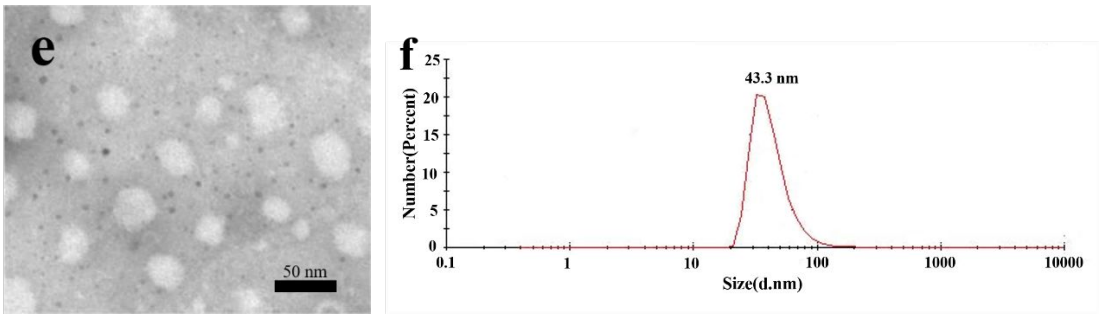

Figure 1. Characterization of P5, CP5 and CLP5. (a) Mass spectrometry of P5 peptide. (b) Mass spectrometry of CP5 peptide. (c) Mass spectrometry of CLP5 peptide. (d)Mass spectrometry of CLP5 peptide. (e) TEM image of CLP5 peptide aggregates. (f) Particle size distribution of CLP5 peptide aggregates.

3.2 Encapsulation and releasing behavior

DOX, as a classic chemotherapy drug, has good anti-tumor effects, but it can cause serious toxic side effects. CLP5@DOX nanomedicine which was prepared by the encapsulating of CLP5 aggregates to DOX can slow down the release of DOX and reduce its toxic side effects. Meanwhile, DOX can be released from the CLP5@DOX nanomedicine which is a prerequisite for its anti-tumor effect. Herein, the encapsulating ratio and release behavior were determined through measuring the drug loading ration and the *in vitro* release experiments. The encapsulation efficiency of CLP5 aggregates to DOX was 81.46±3.23%, and the high encapsulation efficiency ensure that the CLP5@DOX nanomedicine can release sufficient DOX at the tumor site, thereby exert better anti-tumor effects.The unlimited proliferation of tumor cells requires Glycolysis to provide energy, which produces a large amount of lactic acid, leading to the weak acidic microenvironment of tumor tissue. Therefore, the releasing behavior DOX from the CLP5@DOX nanomedicine was conducted under neutral and acid pH conditions. The experimental results were shown in **Figure 2a**. The release rate of DOX from the CLP5@DOX nanomedicine at pH 5.0 was faster than that at pH 7.4, it may be because the depolymerize CLP5 aggregates was faster at pH 5.0 than at pH 7.4, which caused the faster releasing in acid solution than in neutral solution. The release rate of DOX from the CLP5@DOX nanomedicine was faster in PBS containing 10% serum than that of pure PBS as shown in **Figure 2b,** and the reason may be that the serum contains abundant proteases, and the interaction of CLP5 aggregates and protease leads to faster depolymerization of CLP5 aggregates in serum than in pure PBS, which leads to faster

drug release in the serum. Therefore, the DOX release from the CLP5@DOX nanomedicine has the characteristics of pH responsiveness and sustained release, thereby reducing toxic side effects and enhancing anti-tumor effects.

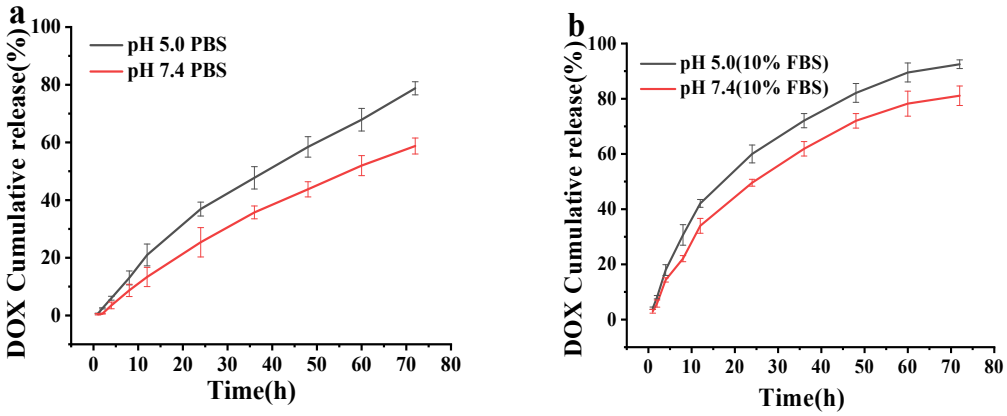

Figure 2. Release of CLP5@DOX nanomedicines at 37°C. (a) Release curves of nanomedicines in phosphate buffer saline at pH 5.0 and pH 7.0. (b) Release curves of nanomedicines in fetal bovine serum at pH 5.0 and pH 7.0.

3.3 *In vitro* anticancer activity and serum stability

The anticancer activities of CLP5 and CLP5@DOX nanomedicine were determined with the MTT method.The relative HepG2 cell viability were shown in **Figure 3a** and **Figure 3b** after the co-culture of HepG2 and the CLP5, CLP5@DOX nanomedicine and DOX for 24 hours and 48 hours respectively. The experimental results showed that with the increase of drug concentration, the relative cell survival rate of cancer cells gradually decreased, and which indicated that the killing effect of drugs to cancer cells became stronger and stronger. The relative survival rate of HepG2 cancer cells was above 80% when the CLP5 concentration was 20 $\mu g \cdot mL^{-1}$ for 48 hours incubation, and when the concentration of CLP5 was 120 $\mu g \cdot mL^{-1}$, the survival rates of cancer cells which was co-cultured with HepG2 cells for 24 hours was 52%, which indicated that the apoptosis of HepG2 cell was CLP5 concentration dependent. CLP5@DOX nanomedicine group and DOX group had the same performance as CLP5 as shown in **Figure 3a** and **Figure 3b,** and the killing effect on cancer cells became stronger with increasing concentration, thus also exhibiting concentration dependence. Compared with the **Figure 3a** and **Figure 3b,** the relative HepG2 cancer cell survival rate

gradually decreased with the time prolongation (24 hours and 48 hours), and which indicated that the apoptosis efficiency of CLP5 group and CLP5@DOX nanomedicine group were time dependent.

Polypeptide drugs are susceptible to be degraded and inactivated by protein hydrolase in serum after entering the body, so high serum stability is a crucial property for ensuring the effectiveness of polypeptide drugs. Firstly, the CLP5 (200 $\mu g \cdot mL^{-1}$) was pre cultured in PBS containing 10% FBS for 24 and 48 hours respectively, and then its anti-cancer activity was determined by MTT method to evaluate its serum stability. Seen from the **Figure 3c,** the relative survival rates of HepG2 cancer cells after co-culturing with CLP5 for 24 hours and 48 hours were 50% and 46% respectively, and the relative survival rates of HepG2 cancer cells after co-culturing with 10% FBS for 24 and 48 hours were 48% and 44% respectively, and which indicated that the serum had little effect on the anticancer activity of CLP5, and there was no significant change in the anticancer ability, which indicated that CLP5 has high serum stability. The high serum stability may be attributed to the concealment of its amino and carboxyl ends. Additionally, the modification of fatty acids further enhances its serum stability.

The cytotoxicity of CLP5 cyclic lipopeptide was shown in **Figure 3d**, and the relative survival rate of RAW 264.7 cells was still greater than 70% when the concentration of CLP5 cyclic peptide reached 200$\mu g \cdot mL^{-1}$, and which indicated that CLP5 cyclic lipopeptide had very low toxicity to normal cells and good safety.

In summary, the toxicity of CLP5 cyclic lipopeptide was very low, and the anticancer activity of CLP5@DOX was concentration and time dependent.

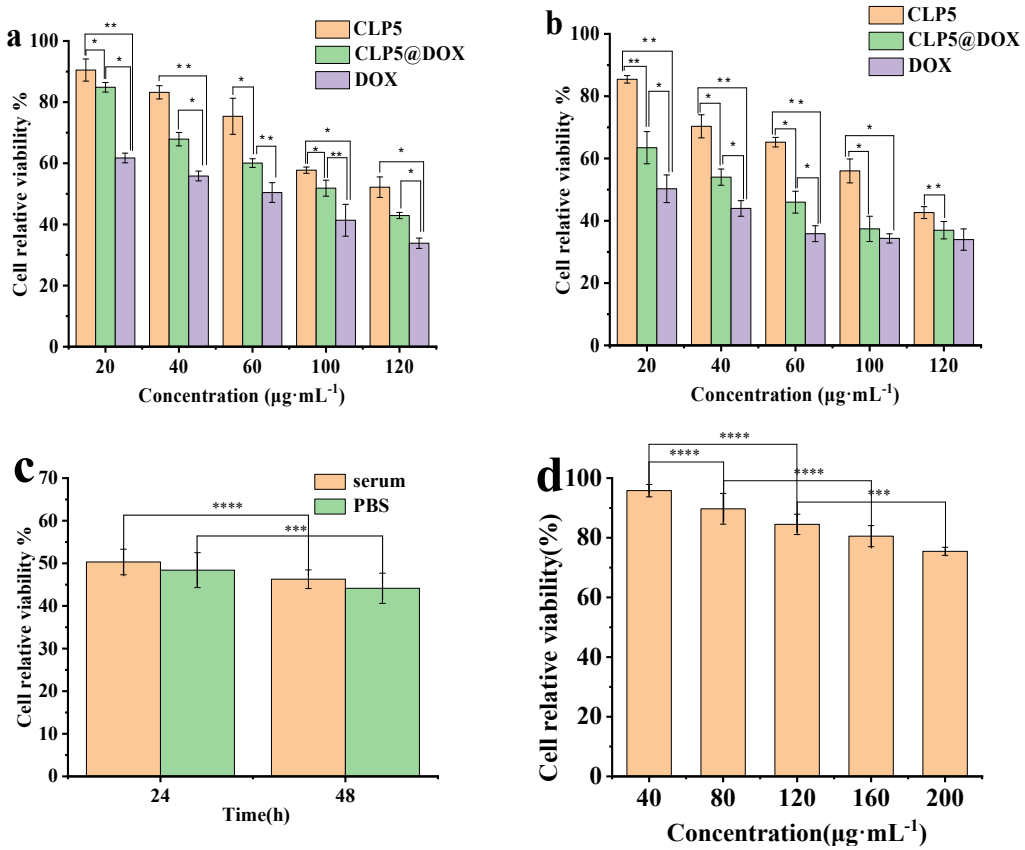

Figure 3. *In vitro* anticancer activity and serum stability. (a) Relative viability of HepG2 cells after co-incubation with different concentrations of CLP5,CLP5@DOX nanomedicine and DOX for 24 h. (b) Relative viability of HepG2 cells after co-incubation with different concentrations of CLP5, CLP5@DOX nanomedicine and DOX for 48 h. (c) Relative viability of HepG2 cells incubated with 120 μg·mL^{-1} CLP5 cyclic lipopeptide in PBS and 10% FBS solution for 24 h and 48 h.(d) Relative cell survival rate after co-culture with RAW 264.7 cells with different concentrations of CLP5 cyclic lipopeptide for 24 h. * $p < 0.05$,** $p < 0.01$, ***$p<0.001$, ****$p<0.0001$.

3.4 Penetrating membrane activity

Hoechst33342 is a nuclear dye that can penetrate the cell membrane and embed into the DNA of cell nuclear, and it can enter the cell in a small amount to make it blue. The permeability of damaged cell membranes is enhanced, and the structure of chromosome DNA is altered, which results in an increase in the amount of Hoechst33342 dye entering, and it make more stable and effective in binding to DNA. The fluorescence intensity increases and appears bright blue. PI can only stain the nucleus of cells with damaged cell membranes, that is, apoptotic and necrotic cells can be stained by PI which make the cell red.

As shown in **Figure 4a** and **Figure 4b**, the cells were blue when co-cultured with

CLP5 and HepG2 cells for 5 minutes (**Figure 4a**), and which indicated that Hoechst33342 dye had entered the cells, but there was almost no red fluorescence (**Figure 4b**), which indicated that PI dye almost did not penetrate the cell membrane into the cells, and the HepG2 cell membrane was intact without damage. **Figure 4c** showed that the cells showed a bright blue color after co-culturing of HepG2 cells with CLP5 for 30 minutes, which was due to the increased membrane permeability of apoptotic cells, and the large amount of Hoechst33342 dye entered the cells, which resulted in increase of fluorescence intensity. Seen from the **Figure 4d**, the HepG2 cells showed red fluorescence, which indicated that the interaction between CLP5 and HepG2 cells for 30 minutes exerted a membrane breaking effect, and lead to the permeability increase. So the CLP5 has good cancer cell membrane breaking activity.

Tumor cells contain abundant LDH which cannot pass through the cell membrane under normal circumstances. When the cell membrane is damaged, it can be released outside the cell. Therefore, the degree of cell damage can be determined by measuring the release rate of LDH. LDH detection kit was used to quantitatively measure the membrane breaking ability of CLP5. The release rate of LDH gradually increases with the increase of CLP5 concentration as shown in **Figure 4e**. When the concentration of CLP5 was 40 $\mu g \cdot mL^{-1}$, the release rate was only 42.99%, and the LDH release rate could reach 82.18% when the CLP5 concentration increased to 200 $\mu g \cdot mL^{-1}$, which indicated that CLP5 had certain membrane breaking activity. In summary, CLP5 exerts anti-tumor effects by disrupting cancer cell membranes in a concentration dependent manner.

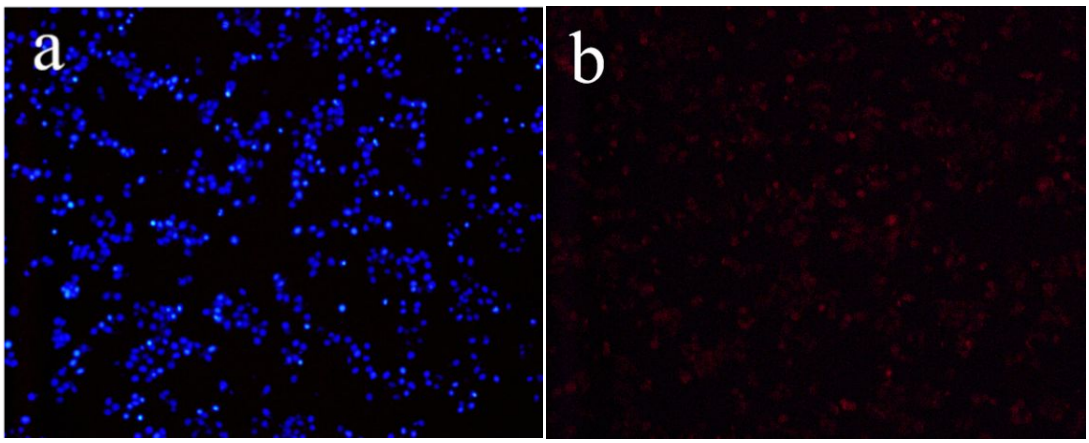

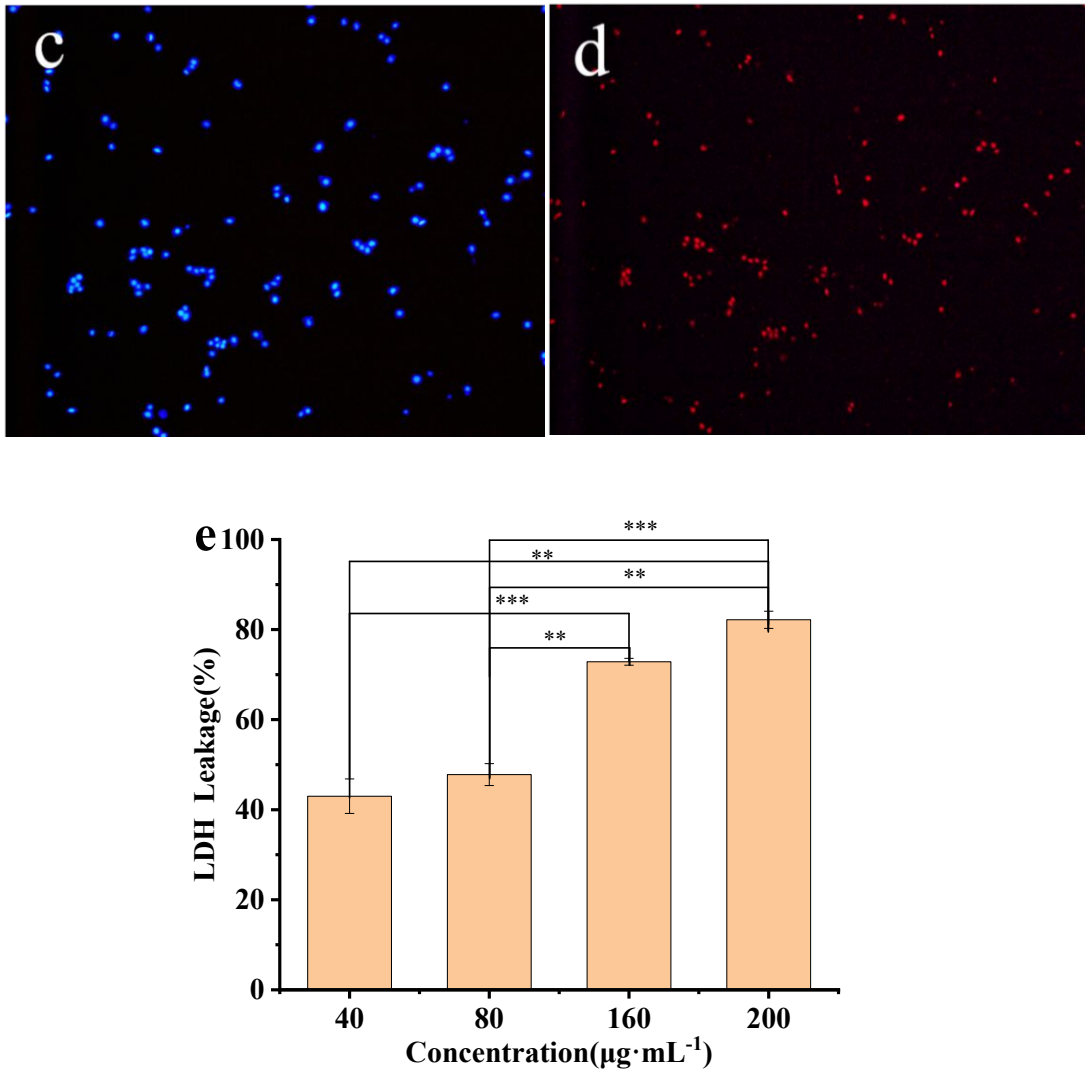

Figure 4. Penetrating membrane activity of the CLP5 cyclic lipopeptide. Fluorescence images of CLP5 cyclic lipopeptide co-incubated with HepG2 cells for 5 minutes (a-b) and 30 minutes (c-d) and then stained with PI/Hoechst 33342 (400×). (e) LDH release content from HepG2 cells incubated with different concentrations of CLP5 cyclic lipopeptide for 24 h, ** $p < 0.01$, ***$p<0.001$.

3.5 Cell uptake

The successful uptake of CLP5@DOX nanomedicine by cancer cells is one of the important indicators for evaluating the performance of CLP5@DOX nanomedicine. Therefore, FCM (**Figure 5a-5d**) was used to quantitatively study the uptake of HepG2 cells to CLP@DOX nanomedicine. Seen from the **Figure 5a-5d**, the fluorescence intensity gradually increased with the increasing time of culturing with HepG2 and CLP5@DOX nanomedicine, which showed that the release amount of DOX from the CLP5@DOX nanomedicine in cells gradually increased, and which indicated that the

CLP@DOX nanomedicine released DOX in a time-dependent manner to exert anti-tumor effects[27-28].

LSCM allows for a more intuitive observation of the uptake of DOX in CLP5@DOX nanomedicine by HepG2 cells. **Figure 5e-5h** showed the uptake of CLP5@DOX nanomedicine after incubation with HepG2 cells. Compared with the control group **Figure 5e**, **Figure 5f** showed that red fluorescence appeared, and which was very weak and mainly concentrated around the cytoplasm, and there was no significant change in cell morphology after 4 hours hours of interaction between CLP5@DOX nanomedicine and HepG2 cells. **Figure 5g** showed that the cells began to deform, and the shape of the cells began to transform from spindle to circular, and the red fluorescence of DOX was significantly enhanced after 8 h of co-culturing with the CLP5@DOX nanomedicine and HepG2 cells. **Figure 5h** showed that the red fluorescence intensity had reached its maximum, and most of the cells had undergone significant changes in shape, transforming from spindle to circular shape. The cells begin to contract and undergo apoptosis after 24 hours of co-culturing with the CLP5@DOX nanomedicine and HepG2 cells. In addition, red DOX fluorescence transfered from the cytoplasm to the nucleus, and a clear red fluorescence appears in the nucleus. The results of LSCM showed that the DOX could be slowly released from the CLP5@DOX nanomedicine into cells, and aggregated into cells, and exerted the anti-tumor effects. The LSCM experimental results were consistent with those of FCM experiments results.

The above experiments indicated that CLP5@DOX nanomedicine could be successfully uptake by cancer cells. The uptake behavior of nanomedicine by cells generally is the endocytosis. The pathways of endocytosis mainly include macroendocytosis, reticulin mediated endocytosis, and caveolin mediated endocytosis. The pathway of CLP5@DOX nanomedicine which entered into the cell was studied with the chlorpromazine (a grid protein dependent endocytosis inhibitor), amiloride (a macrocytosis inhibitor), and methyl-β-Cyclodextrin (an endocytosis inhibitor mediated by caveolin)which were co-cultured with the HepG2 cells.Compared with the positive group(**Figure 5 i**), the uptake of CLP5@DOX nanomedicine was significantly inhibited

by chlorpromazine, and the amiloride also had a certain inhibitory effect, and the methyl-β-Cyclodextrin had not inhibitory effect. The results indicated that the uptake of CLP5@DOX nanomedicine by the HepG2 cells may mainly be achieved through grid protein dependent endocytosis, as well as through certain macrocytosis.

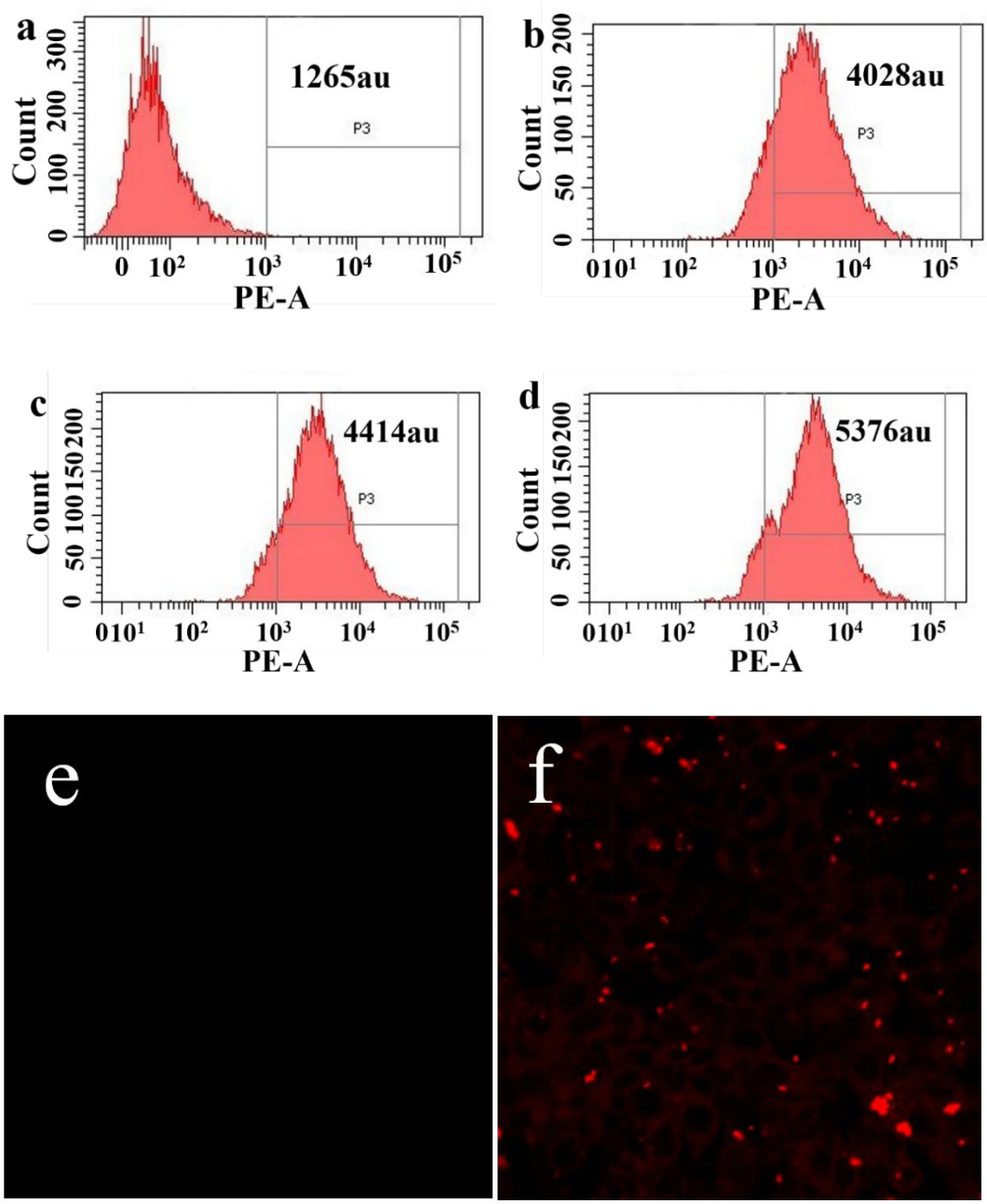

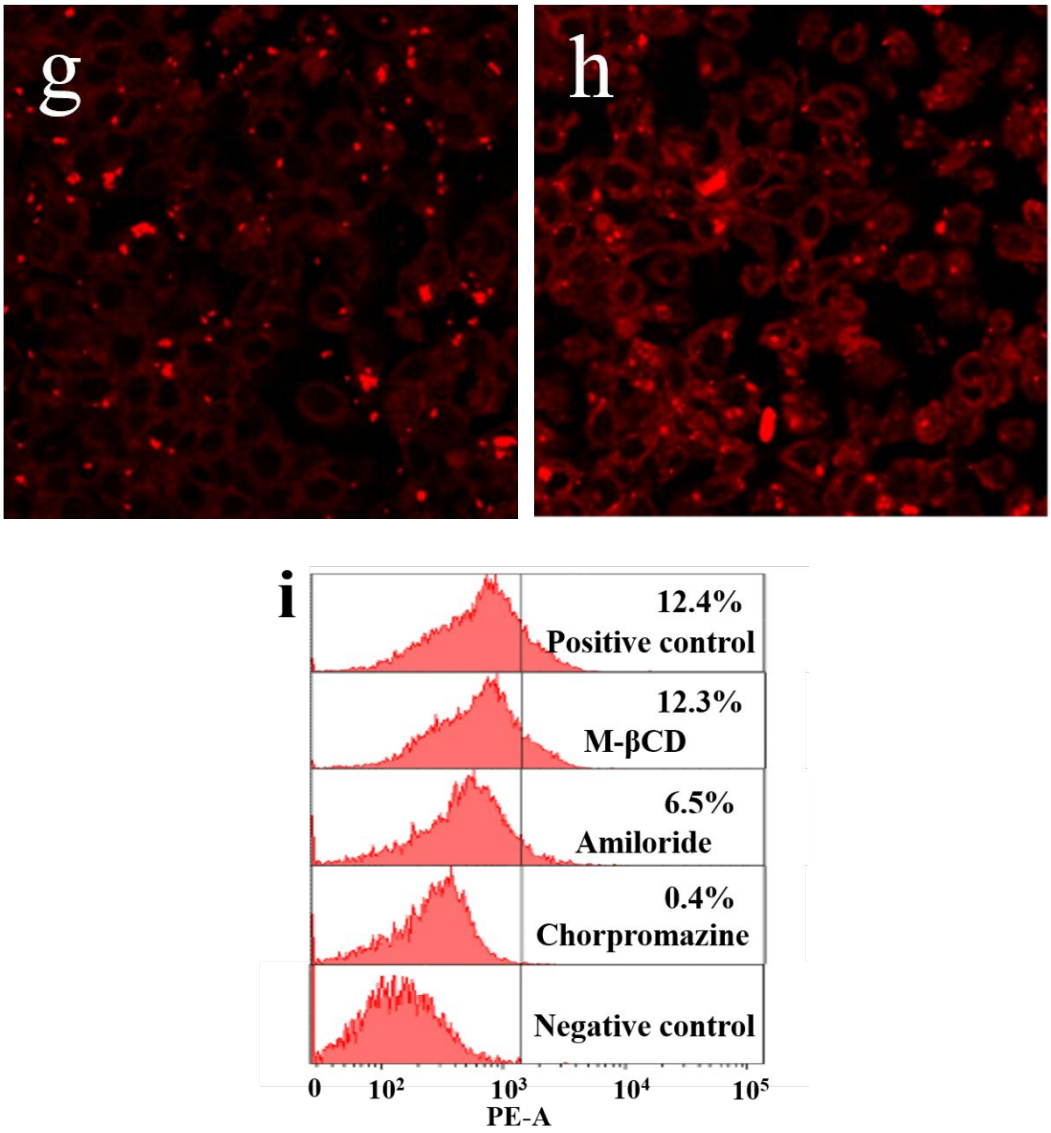

Figure 5. Cellular uptake of 10 μg·mL^{-1} CLP5@DOX nanomedicine. (a) FCM assay of control group. FCM assay of HepG2 cells co-cultured CLP5@DOX nanomedicine for 4 h (b), 8 h (c) and 24 h (d). (e) CLSM assay of control group. CLSM assay of HepG2 cells co-cultured CLP5@DOX nanomedicine for 4 h (f), 8 h (g) and 24 h (h) (400 ×). Effect of inhibitors to uptake of CLP5@DOX nanomedicine by HepG2 cells(i).

3.6 *In vivo* antitumor activity

Tumor bearing mouse model was constructed to study the *in vivo* anti-tumor effects of CLP5 and CLP5@DOX nanomedicine[29-31]. Before the *in vivo* anti-tumor experimental study, the hemolytic experiment was carried out to test the CLP5@DOX nanomedicine. Seen from **Figure 6a-c**, the CLP5 group (**Figure 6b**) and the CLP5@DOX nanomedicine group (**Figure 6c**) showed a disc-shaped, double-sided concave shape of red blood cells at the experiment concentration, and there was no change in morphology compared to the NS group (**Figure 6a**), and which indicated that the CLP5 and

CLP5@DOX nanomedicine at the experiment concentration did not cause hemolysis, so animal experiments could be conducted at the experimental concentration.

Figure 6d showed the change curve of mice body weight with administration time. Seen from the **Figure 6d**, the NS group, CLP5 group, and CLP5@DOX nanomedicine group did not show any significant changes, but there was a slight increase. However, the mice in the DOX group experienced a significant decrease in weight. It could be attributed to the fact that DOX is a broad-spectrum anti-tumor drug that lacks selectivity towards tumor tissue and can cause serious toxic side effects on normal cells while killing cancer cells. The tertiary amine structure of CLP5 can undergo protonation in the tumor environment and interact electrostatically with the negative components of the cancer cell membrane, thereby selectively targeting tumor tissue and reducing side effects on normal tissue.

The original data of tumor volume were shown in **Table S1, Table S2, Table S3** and **Table S4** below, and the changes curve of the mice tumor volume was shown in **Figure 6e**, it could be clearly seen from the **Figure 6e** that the growth rate and volume of tumors in the NS group increased rapidly with time, while in the DOX group and CLP5@DOX nanomedicine group, the tumor growth was significantly slowed down, and the DOX group was the slowest. Seen from the anatomical map of mouse tumors (**Figure 6f**), the NS group had the largest tumor volume, followed by the CLP5 group and the CLP5@DOX nanomedicine group, and the DOX group was the smallest. It indicated that CLP5 had certain anti-tumor abilities, and the CLP5@DOX nanomedicine have pH response release. Therefore, the CLP5@DOX nanomedicine could aggregate at the tumor site, and the DOX was released from the CLP5@DOX nanomedicine when the CLP5@DOX nanomedicine reached the tumor and exerted the anti-tumor effects. In summary, the experimental results indicated that CLP5@DOX nanomedicine could exert the combined anti-tumor effect of DOX and reduce the toxic side effects of DOX.

Tumor bearing mice were euthanized after the experiment, and tumor tissue sections were stained with HE and observed under microscope to further investigate the anticancer effects of CLP5 and CLP5@DOX nanomedicine. The tumor cells in the NS

group have intact morphology and tight arrangement as shown in **Figure 6g**. Compared to the NS group, the tumor cell density of the CLP5 group (**Figure 6h**) decreased, which indicated that CLP5 had certain anti-tumor activity. The cellular changes in the DOX group (**Figure 6i**) and CLP5@DOX nanomedicine group (**Figure 6j**) were more significant with extensive necrosis of the tumor tissue, and nuclear contraction and dissolution, and apoptosis occurring. It suggested that DOX was successfully released from CLP5@DOX nanomedicine to exert anti-tumor effects.

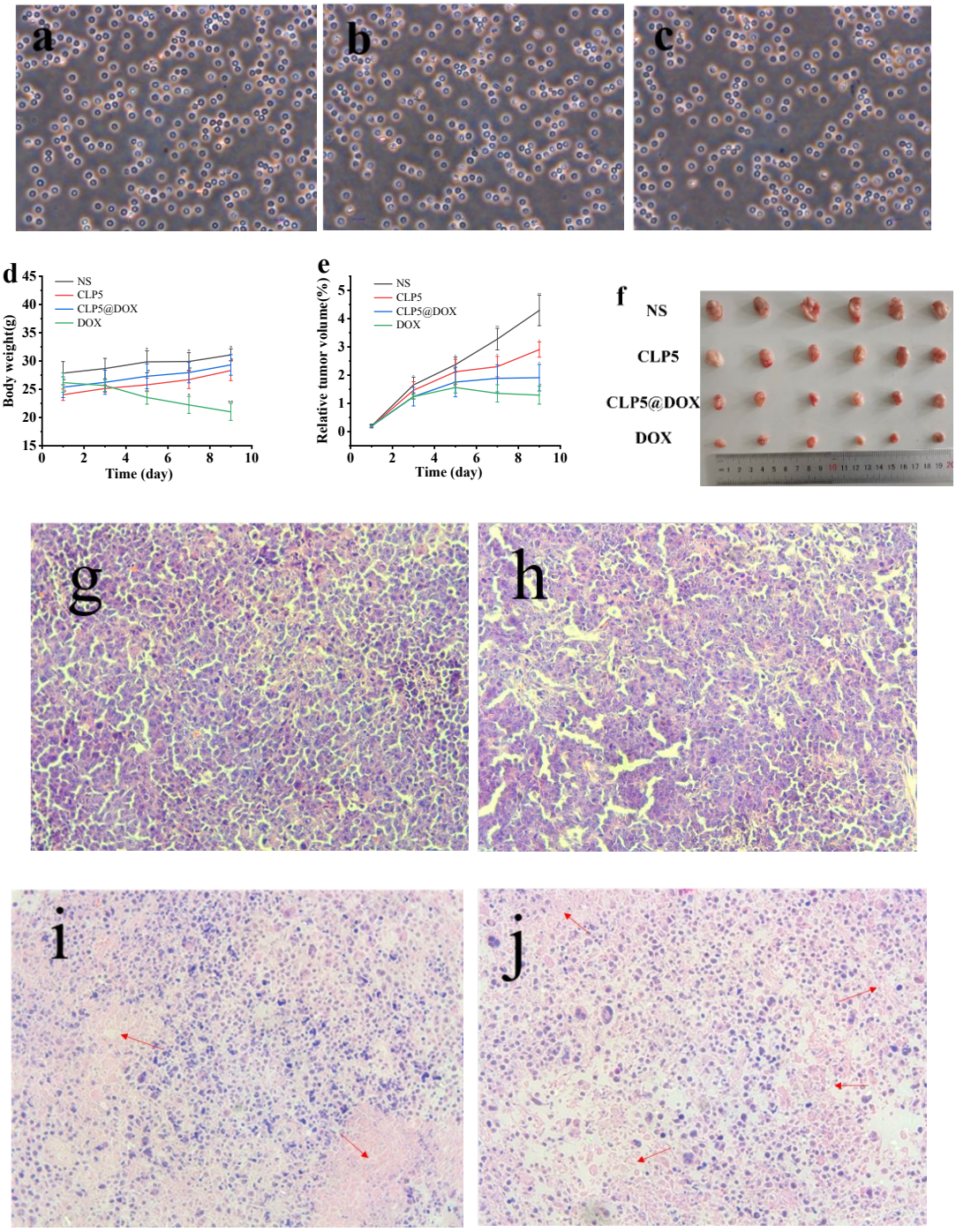

Figure 6. *In vivo* activity assessment of CLP5 and CLP5@DOX nanomedicines. Red blood cell morphology of mice in NS (a), CLP5 (b) and CLP5@DOX (c) groups after 2 h injection(400×). (d) The change of body weight of mice with time. (e) The change of relative tumor volume of mice with time. (f) Tumor dissection of tumor-bearing mice. Tumor tissue sections of NS group (g), CLP5 group (h), DOX group (i) and CLP5@DOX nanomedicine group (j) (200×),and the arrows indicateed thenecrotic part of the tumor section.

The hearts, liver, spleen, lungs, and kidneys of mice were dissected and stained to study the effects of CLP5 and CLP5@DOX nanomedicine on normal tissues and organs. There were no significant differences in the tissues and organs between the NS group, the CLP5 group and the CLP5@DOX nanomedicine group as shown in **Figure 7**, and which indicated that CLP5 and CLP5@DOX nanomedicine had good safety. However, the DOX group showed significant changes of the tissues and organs with significant pyknosis in the spleen of mice, and it indicated that DOX had serious toxic side effects on the tissues and organs of mice. In addition, there was a large amount of ferroflavin deposition in the spleen slices of mice in the DOX group as shown in **Figure 7f,** and which indicated that the toxic side effects of DOX had caused serious damage to the spleen of mice. The ferroflavin was not found in the CLP5 group and CLP5@DOX nanomedicine group, and which indicated that CLP5@DOX nanomedicine could exert anti-tumor effects while reducing the toxic side effects of DOX. In summary, CLP5 can induce the apoptosis of cancer cells through membrane lysis, and also serve as an excellent drug carrier to encapsulate chemotherapy drugs and exert combined anti-tumor effects.

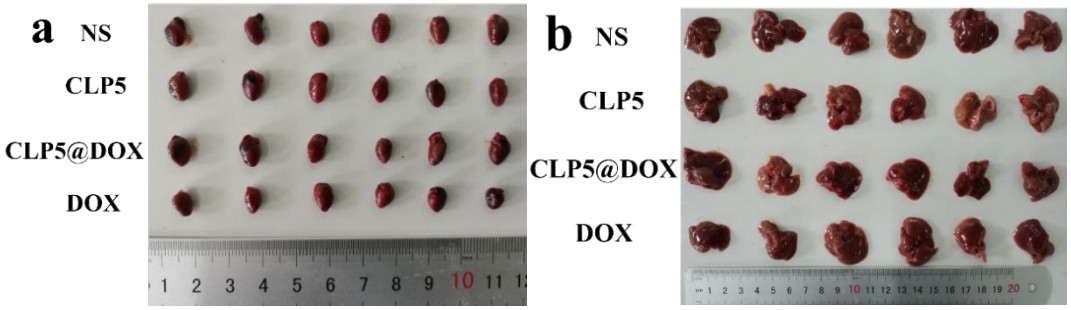

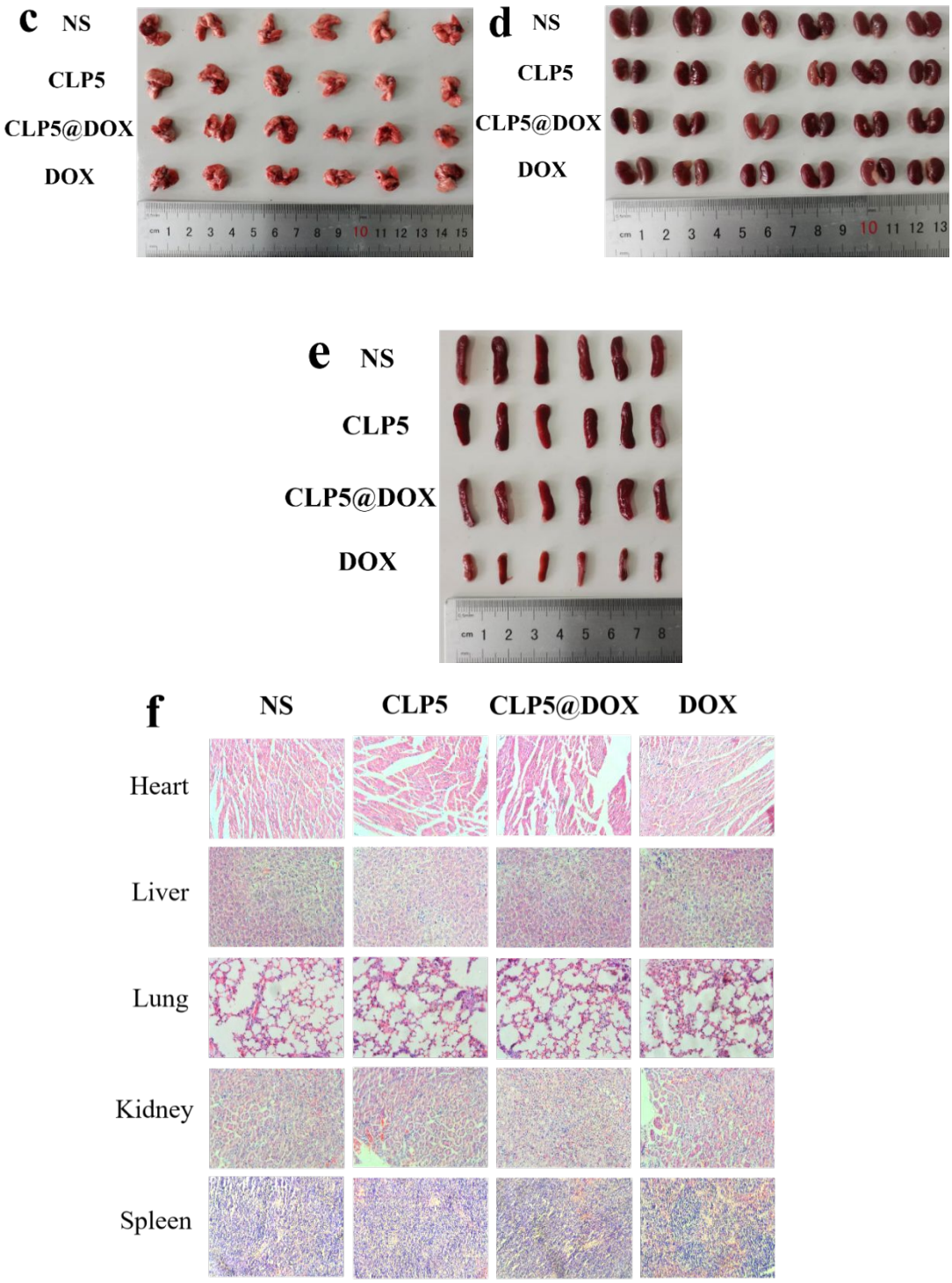

Figure 7. Tissue dissection of tumor-bearing mice. Anatomical pictures of the heart (a), liver (b), lungs (c), kidneys (d) and spleen (e). (f) Tissue sections of heart, liver, spleen, lung and kidney (200×).

3.7 Molecular docking of caspase-3 and CLP5 cyclic lipopeptide

Hydrogen bond interaction is the main reason for the activity of oxadiazole compounds[32]. Therefore, in order to understand the binding mode of CLP5 cyclic lipopeptide and caspase-3, molecular docking experiments were conducted. The results

of molecular docking were shown in **Figure 8a** and **Figure 8b**, and the CLP5 bond to caspase-3 through four hydrogen bonds, and which activated caspase-3 and induced cancer cell apoptosis. The first hydrogen bond was formed between the oxygen atom of 1,3,4-oxadiazole and ARG-341 of caspase-3 with 1.9 Å distance (**Figure 8b**). The second hydrogen bond was formed between the nitrogen atom of glycine and the SER-339 of caspase-3 with 3.0 Å distance. The third hydrogen bond was formed between the double bond oxygen of phenylalanine and TYR-338 of caspase-3 with a distance of 2.4 Å. The fourth hydrogen bond was formed between the double bond oxygen on the side chain of the CLP5 and the PHE-381B of caspase-3 with a distance of 2.8 Å. The above molecular docking results indicated that CLP5 could exert anti-tumor effects by activating the caspase-3 to target apoptosis pathway. Furthermore, molecular docking results were consistent with the cell and animal experiments.

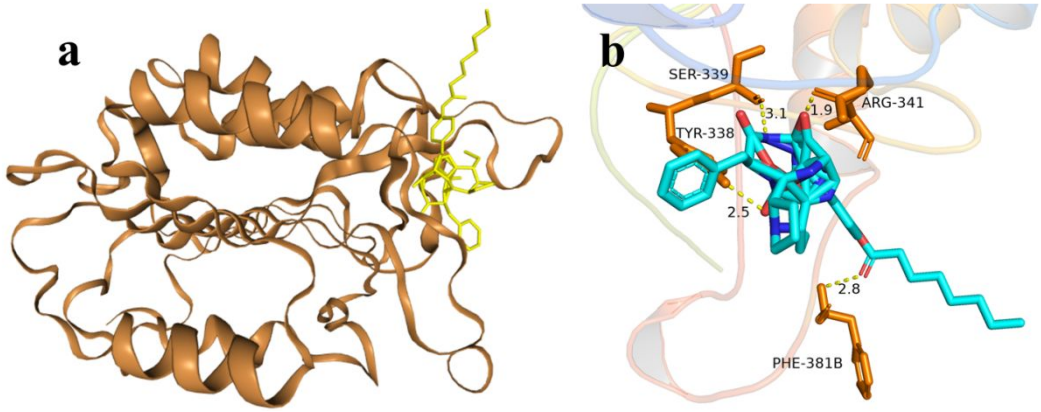

Figure 8. Molecular docking results of caspase-3 and CLP5 cyclic lipopeptide.

4. Conclusion

Herein, a cyclic lipopeptide CLP5 which contained both 1,3,4-oxadiazole and tertiary amine structures was synthesized with certain penetrating membrane activity and high serum stability. CLP5 could self-assemble into spherical aggregates in aqueous solution, which could encapsulate DOX to form CLP5@DOX nanomedicine with high DOX loading rate. The DOX release from the CLP5@DOX nanomedicine was sustained release and pH responsiveness. Cell experiments showed that CLP5 not only had high safety but also had certain membrane permeability. CLP5@DOX nanomedicine could be effectively uptake by cancer cells and induced cancer cell apoptosis. Animal experiments showed that CLP5 aggregates had certain anti-tumor activity,

CLP5@DOX nanomedicine could significantly reduce the toxic side effects of DOX while exerting anti-tumor effects. Molecular docking experiments had revealed that CLP5 targeted caspase-3 to induce apoptosis of cancer cells. In summary, CLP5 aggregates are an ideal drug carrier, and the CLP5@DOX nanomedicine has the application potential in cancer treatment.

5. Author contributions

Conceptualization: Miaomiao Yan and Guangcheng Wei. Data curation: Wenjie Zhang, Junlin Luo. Formal Analysis: Wenjie Zhang. Funding acquisition: Miaomiao Yan and Guangcheng Wei. Investigation: Wenjie Zhang. Methodology: Miaomiao Yan and Guangcheng Wei. Project administration: Miaomiao Yan and Guangcheng Wei. Resources: Miaomiao Yan and Guangcheng Wei. Software: Wenjie Zhang, Junlin Luo, Miaomiao Yan and Guangcheng Wei. Supervision: Miaomiao Yan and Guangcheng Wei. Validation: Wenjie Zhang, Junlin Luo, Jingyang Sun, Weixi Chen, Miaomiao Yan, Guangcheng Wei. Visualization: Wenjie Zhang. Writing - original draft: Wenjie Zhang, Miaomiao Yan and Guangcheng Wei. Writing - review & editing: Wenjie Zhang, Junlin Luo, Jingyang Sun, Weixi Chen, Miaomiao Yan, Guangcheng Wei. All authors have given approval to the final version of the manuscript.

6. Conflicts of Interest

There are no conflicts of interest to declare.

7. Acknowledgements

This study was financially supported by Shandong Provincial Natural Science Foundation, China (Grant No. ZR2023MB141 and ZR2022MB001), and Yantai Technology Innovation Center of Bioactive Peptides（2024KCPT013）, and Projects of medical and health technology development program in Shandong province, China (Grant No.202213050393), and NSFC (Grant No. 21201020), and Key Support projects (Inheritance and development of traditional Chinese Medicine) of the State Administration of Traditional Chinese Medicine, and Key Research and Development Plan of Yantai (No.2018XSCC050), and 2021 New Coronavirus Cultivation Project (Grant No. BY2021XGFY02), and the College Students' Innovation Project of Shandong Province (Grant No. 202310440229 and No. S202310440095), and Yantai

Medical Antibacterial Material Innovation Service Platform.

8. Ethical statement

All animal procedures were performed in accordance with the Guidelines for Care and Use of Laboratory Animals of Binzhou Medical University and approved by the Animal Ethics Committee of Binzhou Medical University.

Reference

[1] Soerjomataram I, Bray F. Planning for tomorrow: global cancer incidence and the role of prevention 2020-2070. *Nature reviews Clinical oncology*. **2021**, 18(10):663-672.

[2] Siegel RL, Miller KD, Fuchs HE, et al. Cancer statistics, 2022. *CA Cancer J Clin*. **2022**, 72(1):7-33.

[3] Galmarini D, Galmarini CM, Galmarini FC. Cancer chemotherapy: a critical analysis of its 60 years of history. *Critical Reviews in Oncology/Hematology*, **2012**, 84(2):181-199.

[4] Tamargo J, Caballero R, Delpón E. Cancer chemotherapy and cardiac arrhythmias: a review. *Drug safety*. **2015**, 38(2):129-152.

[5] Sarafraz-Yazdi E, R Pincus M, Michl J. Tumor-targeting peptides and small molecules as anti-cancer agents to overcome drug resistance. *Current Medicinal Chemistry*. **2014**, 21(14):1618-1630.

[6] Liu X, Wu F, Ji Y, et al. Recent advances in anti-cancer protein/peptide delivery. *Bioconjugate Chemistry.* **2018**, 30(2):305-324.

[7] Karami Fath M, Babakhaniyan K, Zokaei M, et al. Anti-cancer peptide-based therapeutic strategies in solid tumors. *Cellular & Molecular Biology Letters.* **2022**, 27(1):33.

[8] Wu C, Wang M, Sun J, et al. Peptide-drug co-assembling: A potent armament against cancer. *Theranostics.* **2023**, 13(15):5322.

[9] Tsutsumi H, Kuroda T, Kimura H, et al. Posttranslational chemical installation of azoles into translated peptides. *Nature Communications*. **2021**, 12(1):696-697.

[10] Vaidya A, Pathak D, Shah K. 1,3,4-oxadiazole and its derivatives: A review on recent progress in anticancer activities. *Chem Biol Drug Des*. **2021**, 97(3):572-591.

[11] Frost JR, Scully CC, Yudin AK. Oxadiazole grafts in peptide macrocycles. *Nature Chemistry*. **2016**, 8(12):1105-1111.

[12] Appavoo SD, Kaji T, Frost JR, Scully CCG, Yudin AK. Development of Endocyclic Control Elements for Peptide Macrocycles. *Journal of the American Chemical Society*. **2018**, 140(28):8763-8770.

[13] Soor HS, Appavoo SD, Yudin AK. Heterocycles: Versatile control elements in

bioactive macrocycles. *Bioorganic & Medicinal Chemistry*. **2018**, 26(10):2774-2779.

[14] Taechalertpaisarn J, Ono S, Okada O, Johnstone TC, et al. A New Amino Acid for Improving Permeability and Solubility in Macrocyclic Peptides through Side Chain-to-Backbone Hydrogen Bonding. *Journal of medicinal chemistry*. **2022**, 65(6):5072-5084.

[15] Boudreau MW, Peh J, Hergenrother PJ. Procaspase-3 Overexpression in Cancer: A ParaDOXical Observation with Therapeutic Potential. *ACS chemical biology*. **2019**, 14(11):2335-2348.

[16] El Mansouri AE, Oubella A, Mehdi A, et al. Design, synthesis, biological evaluation and molecular docking of new 1,3,4-oxadiazole homonucleosides and their double-headed analogs as antitumor agents. *Bioorganic Chemistry*. **2021**, 108, 104558.

[17] Boudreau MW, Peh J, Hergenrother PJ. Procaspase-3 Overexpression in Cancer: A ParaDOXical Observation with Therapeutic Potential. *ACS chemical biology*. **2019**, 14(11):2335-2348.

[18] Huo Y, Ma L, Zhang M, et al. Development of anticancer peptides with low hemolysis, high penetrating membrane activity, certain analgesic activity and the synergistic anticancer effect. *Biomaterials Science*. **2022**, 10(7):1724-1741.

[19] Wallace KB, Sardão VA, Oliveira PJ. Mitochondrial Determinants of doxorubicin-Induced Cardiomyopathy. *Circulation research*. **2020**, 126(7):926-941.

[20] Prakash J, de Jong E, Post E, et al. A novel approach to deliver anticancer drugs to key cell types in tumors using a PDGF receptor-binding cyclic peptide containing carrier. *Journal of controlled release*. **2010**, 145(2):91-101.

[21] Yang Y, Zhao Q, Peng Z, et al. A GSH/CB Dual-Controlled Self-Assembled Nanomedicine for High-Efficacy doxorubicin-Resistant Breast Cancer Therapy. *Frontiers in pharmacology*. **2022**, 12, 811724.

[22] Kuang H, Ku SH, Kokkoli E. The design of peptide-amphiphiles as functional ligands for liposomal anticancer drug and gene delivery. *Advanced drug delivery reviews*. **2017**, 110, 80-101.

[23] Panigrahi B, Singh RK, Mishra S, et al. Cyclic peptide-based nanostructures as efficient siRNA carriers. *Artificial Cells, Nanomedicine, and Biotechnology*. **2018**, 46(sup3):S763-S773.

[24] Kwon YU, Kodadek T. Quantitative comparison of the relative cell permeability of cyclic and linear peptides. *Chemistry & biology*. **2007**, 14(6):671-677.

[25] Song Q, Cheng Z, Kariuki M, et al. Molecular Self-Assembly and Supramolecular Chemistry of Cyclic Peptides. *Chemical Reviews*. **2021**, 121(22):13936-13995.

[26] Ma L, Niu M, Ji Y, et al. Development of KLA-RGD integrated lipopeptide with the effect of penetrating membrane which target the $\alpha_v\beta_3$ receptor and the application of combined antitumor. *Colloids Surf B Biointerfaces*. **2023**, 223, 113186.

[27] Qin L, Cheng X, Wang S, et al. Discovery of Novel Aminobutanoic Acid-Based ASCT2 Inhibitors for the Treatment of Non-Small-Cell Lung Cancer. *Journal of medicinal chemistry*. **2024**;67(2):988-1007.

[28] Liu Y, Zhang D, Zhang Z, et al. Multifunctional nanoparticles inhibit tumor and tumor-associated macrophages for triple-negative breast cancer therapy. *Journal of colloid and interface science*. **2024**,657,598-610.

[29] Fayn S, King AP, Gutsche NT, et al. Site-Specifically Conjugated Single-Domain Antibody Successfully Identifies Glypican-3-Expressing Liver Cancer by Immuno-PET. *Journal of nuclear medicine : official publication, Society of Nuclear Medicine*. **2023**,64(7):1017-1023.

[30] Huang C, Zhou Y, Feng X, et al. Delivery of Engineered Primary Tumor-Derived Exosomes Effectively Suppressed the Colorectal Cancer Chemoresistance and Liver Metastasis. *ACS Nano*. **2023**,17(11):10313-10326.

[31] Zhou C, Weng J, Liu C, et al. Disruption of SLFN11 Deficiency-Induced CCL2 Signaling and Macrophage M2 Polarization Potentiates Anti-PD-1 Therapy Efficacy in Hepatocellular Carcinoma. *Gastroenterology*. **2023**,164(7):1261-1278.

[32] Carbone D, Parrino B, Cascioferro S, et al. 1,2,4-Oxadiazole Topsentin Analogs with Antiproliferative Activity against Pancreatic Cancer Cells, Targeting GSK3β Kinase. *ChemMedChem*. **2021**, 16(3):537-554.

Data availability statement

All relevant data are within the manuscript and its Supporting Information files.